

# Data Decoupling for Efficient Auto-Calibrating Parallel Imaging for Arbitrary Cartesian k-space Sampling: Application to Highly-Accelerated 3D Cardiac Cine MRI

Peng Lai<sup>1</sup>, and Anja C.S Brau<sup>1</sup>

<sup>1</sup>Global Applied Science Laboratory, GE Healthcare, Menlo Park, CA, United States

**Introduction:** Auto-calibrating parallel imaging (acPI) requires a calibration step to generate coil weights for each data synthesis pattern and becomes computationally challenging for acquisition with a large number of patterns (e.g. variable density acceleration, random sampling). Methods such as GRAPPA operator<sup>[1]</sup> can address the computation challenge but considerably degrade image quality at high acceleration factors. We develop a source data decoupling method with two-step calibration that can significantly reduce acPI computation complexity for non-uniform Cartesian sampling with improved reconstruction compared to conventional GRAPPA operator based methods and this work demonstrates its feasibility on 3D cardiac cine MRI using kt GRAPPA<sup>[2]</sup>.

**Theory:** In cardiac cine MRI, due to heart-rate variations during a scan, acquired data must be re-sorted along time based on cardiac signals to reduce motion blurring and for complete-cardiac-cycle motion depiction. Furthermore, variable density acceleration is often used for better tradeoff between scan time and spatiotemporal resolution. Retrospective cardiac gating<sup>[3]</sup> of such k-t datasets with time-interleaved acquisition generates variable-density pseudo-random k-space sampling with a typical number of synthesis patterns ( $N_p$ ) of >500 per time frame. Conventional kt GRAPPA (ktG) performs data synthesis using a 4D kernel ( $k_x-k_y-k_z-t$ ) and calculates coil weights ( $W$ ) for each pattern by fitting a source data matrix ( $A_s$ ) to a target data matrix ( $A_t$ ) using  $W=(A_s^H A_s + \lambda I)^{-1} A_s^H A_t$ , where  $\lambda$  is the regularization parameter. Each such pseudo-inversion involves  $O(N_s^3)$  complex multiplications ( $N_s$ : the total number of source data for a pattern). With large  $N_p$ 's and coil channel numbers ( $N_c$ ), ktG would be prohibitively expensive for online reconstruction.

We develop a source data decoupling method for ktG, referred to as d-ktG, to address this challenge. Fig.1 demonstrates d-ktG calibration in 2D for a pattern with 3 source k-t lines (numbered black dots) and a target at center (empty circle). In calibration, source data of a pattern are decoupled into k-t groups and each group consists of all  $k_x$  neighbors from all coils with a unique  $k_y-k_z-t$  shift. Coil weights are generated using the following two-step calibration: **Step 1:** Find optimal weights ( $W_{1,n}$ ) to fit each k-t group ( $A_{s,n}$ ) to the target dataset using Eq.1:  $W_{1,n}=(A_{s,n}^H A_{s,n} + \lambda I)^{-1} A_{s,n}^H A_t$  and then generate a synthetic target ( $T_{s,n}$ , gray dots in Fig.1) using Eq.2:  $T_{s,n} = A_{s,n} W_{1,n}$ .  $T_{s,n}$  in other words provides exactly the synthetic calibration data generated from the  $n$ th k-t group and thus can be used to optimize combination of syntheses from different k-t groups; **Step 2:** Find the optimal weights ( $W_{2,m}$ ) to recombine all  $T_{s,n}$ 's using Eq.3 below on a coil-by-coil basis to generate the final reconstruction (solid black dots in Fig.1) and combine  $W_1$  and  $W_2$  to generate the final coil weights ( $W=W_1 W_2$ ) for each source datum. Eq.3:  $W_{2,m}=(A'_{s,m}^H A'_{s,m} + \lambda \Phi_m)^{-1} A'_{s,m}^H A_t$ , where  $A'_{s,m}$  is the synthetic source matrix comprised of data from  $T_{s,n}$ 's of the  $m$ -th coil,  $\Phi_m = \text{diag}(W_{1,n}^H \Psi W_{1,n})$  represents noise covariance among  $T_{s,n}$ 's after  $W_1$  data fitting,  $\Psi$  is the original noise covariance of receiver coils and is set to  $I$  in this work. For data synthesis, each missing k-space line is synthesized using  $W$  of the local pattern in one step, similar to ktG.

d-ktG substantially reduces the expensive  $O(N_s^3)$  computation per pattern of ktG to much cheaper  $O(N_s^3)$  and  $O(N_{s2}^3)$  in the above two step calibration, where  $N_{s2}=N_{s1} N_{s2}$ . To further speed up d-ktG, a preparation step can be performed that calculates  $W_{1,n}$ 's for all potential k-t shifts ( $< \text{acceleration}^2$ ) in all synthesis patterns. Then, the computation that needs to be repeated for each pattern involves only inversion of very small matrixes ( $\sim 16 \times 16$  per coil) in step 2. d-ktG fully uses all available source data in each k-t group for data fitting of step 1. Also, using Eq.3, d-ktG regularizes noise

amplification based on noise covariance of synthetic targets and finds the optimal solution with min  $L_2$ -norm errors in the entire space spanned by all synthetic targets. Therefore, d-ktG can potentially provide more accurate reconstruction with higher SNR compared to conventional GRAPPA operator based methods<sup>[1,4,5]</sup>.

**Methods & Material:** To validate the proposed algorithm, we collected 3D cine datasets at 1.5T (GE Healthcare) from 4 volunteers using 8-ch and another 3 volunteers using 32-ch cardiac coils. k-space was sampled in a time-interleaved fashion with 6x outer & 2x center acceleration for 8-ch and 8x outer & 3x center acceleration for 32-ch. Typical imaging parameters included:  $\sim 2 \times 2 \text{ mm}^2$  resolution, 24 slices with 5mm thickness, 48ms temporal resolution. Each dataset was processed using conventional ktG, d-ktG and a GROG-like algorithm (combining syntheses at the same target location after first-step d-ktG using simple averaging<sup>[5]</sup>). In all reconstructions, central k-space was recovered first at each cardiac phase separately using sliding-window to generate calibration data<sup>[6]</sup> and next the fully recovered central k-space was used for calibration in kt reconstruction in outer k-space. An adaptive time-window selection scheme<sup>[7]</sup> was used to determine the temporal neighborhood for each specific cardiac phase. To assess the improvement in computation efficiency, we also analyzed the number of complex multiplications of d-ktG calibration with regard to ktG with uniform and nonuniform kt sampling assuming 8x acceleration,  $k_x$  kernel width of 5 and calibration size of  $50 \times 16 \times 16$  in  $[k_x, k_y, k_z]$ . A correlation coefficient method<sup>[8]</sup> was used to reduce computation of  $A_s^H A_t$  and  $A_s^H A_s$  for all methods wherever beneficial.

**Results:** Table 1 shows that d-ktG dramatically reduces ktG computations, especially for larger  $N_c$ 's and  $N_p$ 's. For instance, for 3D cardiac cine MRI with 32ch ( $N_p=500$  to 1000), d-ktG calibration is  $\sim 300$  to 600 times more efficient than conventional ktG. Furthermore, d-ktG is multiple times faster than ktG on regular sampling datasets with a minimum  $N_p$  of acceleration-1 and increasing  $N_p$  adds only trivial increase in d-ktG computation. Fig.2 shows two representative cases with different accelerations and coils. Clearly, d-ktG (Fig.2.b&e) provides high image quality very similar to ktG (Fig.2.a&d). In comparison, the GROG-like method (Fig.2.c&f) generates visible ghosting artifacts (indicated by arrows) and significantly lower SNR due to its suboptimal combination of syntheses.

**Conclusion:** d-ktG can dramatically improve computation efficiency of ktG especially with large  $N_p$ 's and  $N_c$ 's without sacrificing image quality and is promising for online reconstruction for 3D cardiac cine MRI. This work also develops a novel approach for optimal combination of syntheses from different source data groups. Our in vivo results show that our approach provides higher SNR and reconstruction accuracy than conventional GROG-like methods. The proposed decoupling method can also be used for static 3D MRI by simply removing the time dimension. The high quality results obtained from this work, in which central k-space was reconstructed similar to tGRAPPA without temporal neighbors, suggest that the decoupling method will perform well for static 3D MRI datasets as well.

**References:** [1] Griswood M, MRM 2005, 54:1553; [2] Huang F, MRM 2005, 54:1172; [3] Lai P, ISMRM 2011:3378; [4] Blaimer M, MRM, 2006, 56:1359; [5] Seiberlich N, MRM 2007, 58:1257; [6] Breuer FA, MRM 2005, 53:981; [7] Lai P, ISMRM 2009:766; [8] Beatty P, ISMRM 2007:1749

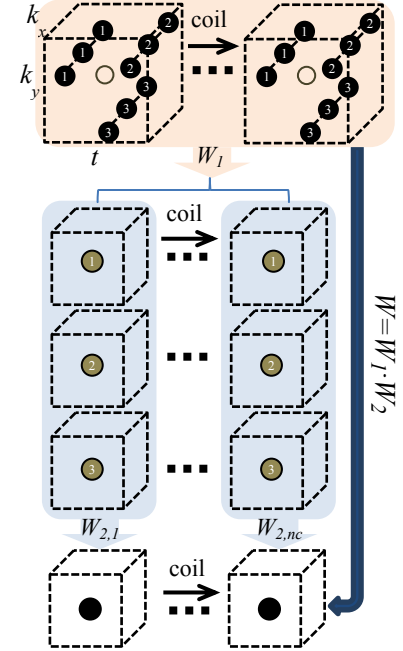


Fig. 1 2D d-ktG calibration flow chart

Table 1. d-ktG computation reduction for different  $N_p$ 's vs. ktG with  $N_p=7$  (R1) & same  $N_p$ 's (R2)

Patterns	50	250	500	750	1000
R1 8ch	8.6×	8.6×	8.5×	8.5×	8.5×
R132ch	13.0×	12.9×	12.9×	12.9×	12.9×
R2 8ch	62×	90×	124×	159×	193×
R2 32ch	78×	183×	313×	443×	573×

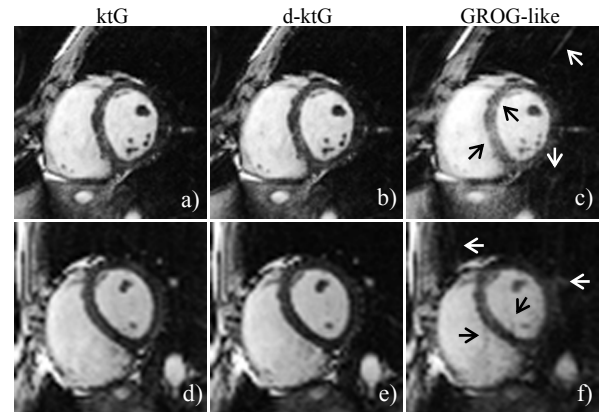


Fig.2 Comparison of reconstructions in 2 cases. Top row: 8ch with 6x outer & 2x center; bottom row: 32ch with 8x outer & 3x center